Impact of gap-graded cement blending on strength, permeability and CO_2 footprint of concrete

P. Stroeven

Faculty of Civil Engineering and Geosciences, Delft University of Technology, the Netherlands

Partial replacement of Portland cement by pozzolanic mineral admixtures exerts direct positive effects on the CO_2 footprint of concretes. The low CO_2 footprint is reinforced by making use of incinerated specific organic waste, such as rice husks, resulting in rice husk ash (RHA). In this way, the CO_2 footprint of obtained concrete is improved. A gap-graded binder leads to improved particle packing density with RHA as the finer component (the filler function), so that high strength concretes can be produced. This is reinforced by the pozzolanic nature of the RHA. Characteristics of the capillary pores developed in the hydrating binder have impact on the transport-based durability properties. Yet, their assessment constitutes a complicated problem, especially in experimental approaches. Therefore, this paper applies a relatively new economic and reliable approach to conduct such investigations on computer simulated (virtual) particulate materials. Application demonstrates the favorable impact of gap-graded blending on pore characteristics relevant for transport related phenomena. The involved reduction in permeability of the uncracked material will therefore promote this aspect of durability, being an essential element of the environmental footprint.

Keywords: Cement, blending, CO_2 footprint, computer simulation, gap-grading, porosimetry, strength, durability

1 Introduction

Portland cement (PC) production contributes by about 6% to global CO_2 emissions. One of the obvious contributions to reducing detrimental effects of Portland cement production on global warming as a result of CO_2 emissions is to reduce the PC content significantly by blending with supplementary cementitious materials (SCMs). Use of a SMC of vegetable

origin, such as RHA, will additionally contribute to waste management and energy conservation [1]. Experimental research with Vietnamese participation, performed at Delft University of Technology (DUT) in the period around the millennium break, exploited successfully the gap-grading particle packing principle (improving particle packing density by combining distinct particle size ranges) by designing such aggregates (very fine sand and coarse aggregate) as well as binders (Portland cement (PC) blended by rice husk ash, diatomite earth or metakaolin) [1 - 4]. In [5, 6] it was shown that PC binders blended with an inert admixture (carbon black, so, just functioning as filler) also resulted in proper strength levels provided the blend was gap-graded, revealing the crucial importance of particle packing. A new series of Vietnamese PhD students later advanced this topic at DUT [7 - 10].

Particle packing is an issue receiving major attention in physics and mathematics. Recognition that it has impact on concrete is also going back to the beginning of previous century. This may be exemplified by an old simple compression test on *cement paste* specimens. Test-loaded specimens were after crushing completely ground down. Thereupon, the mold was filled with this material and compacted by compressive forces. Test-loading demonstrated compressive strength level recovered. This is the particle packing effect in *optima forma*; strength is due to van der Waals forces. Nowadays, separate gap-graded grain fractions are used in the design of Super High-Performance Concretes and of Engineered Cementitious Composites [11].

Experimental research is time-consuming, labor-intensive and thus expensive. Produced data are mostly also biased to an unknown degree [12, 38]. As a result, doing research on virtual material is gaining in popularity in concrete technology. The Discrete Element Method (DEM) definitely offers the most reliable approach for simulating particle dispersion in concrete [12]. Yet, various random sequential addition (RSA) systems are in vogue in the concrete technology field (for a survey, see [13]), which simulate particle dispersion in a biased way, as extensively discussed in [12]. DEM incorporates particle interference, a phenomenon characteristic for the dense quasi-randomly packed aggregate and binder particles, particularly in the High-Performance Concrete (HPC) range. At DUT, we have executed among others studies with Chinese and Vietnamese participation on meso- as well as on micro-level of the virtual material using the DEM systems SPACE and HADES [14 - 18]. The favorable and well-known effect of gap-grading on strength found in the aforementioned Vietnamese-Dutch experimental research was confirmed.

Recent DEM studies of (blended) PC have focused among other things on the pore network structure as affected by gap-grading. The interpretation of the first test series with SPACE [16] seemed conforming to the concept for soil materials of Vogel and Roth [19]. For concrete, this would imply the development during hydration of continuous pores around aggregate grains that could mutually connect in (partly) percolated Interfacial Transition Zones (ITZs). The inkbottle effects that are hypothesized for pore structures in concrete could be associated with incomplete connections in the overlap zones. The most recent ongoing investigations by HADES [20, 21] also reveal the pore trees particularly concentrated in ITZs, however with branching pores that form connections outside ITZs in the so-called bulk regions that form a significant part of the matured paste in concrete. As a consequence, the peak value in the connected pore fraction near the aggregate grain surfaces was concluded not dominating the global value of connected porosity of concrete [22]. Hence, the degree of ITZ percolation cannot be expected to dominantly govern chloride diffusion [23]. Moreover, partial water saturation conditions in practice will significantly reduce the differences between bulk and ITZ as to relevant porosity characteristics [24 - 26].

The favorable effects on the pore network structure by gap-graded blending and the implications for mechanical properties were convincingly revealed [20,21] and will be shortly mentioned herein. Yet, the prime objective of this paper is the extension of the favorable packing effects to pore characteristics relevant for permeability of fully water saturated concrete obtained by DEM-produced 'compucrete'. This will have consequences for designing concretes with low CO_2 footprint.

2 Methodology of virtual material simulation

2.1 Simulation of fresh blended cement paste by DEM (HADES)

To obtain matured virtual cement paste, firstly, the fresh cement particles need to be generated. In this research, packing of fresh cement particles is simulated by HADES (HAbanera's Discrete Element Simulator). HADES is an advanced dynamic force-based DEM system for making realistic packing simulations of arbitrarily shaped particles. This could be the aggregate on meso-level or the binder on micro-level [12, 27, 28].

Mechanical interaction in HADES is based on a contact mechanism algorithm that evaluates the interaction forces exerted between segments of tessellated surfaces of

neighboring particles. The contact forces are functions of distances and of activated areas of the segments. Several forces can be applied in this way on a particle such as spring force, cohesion force, damping force and friction force. HADES renders possible implementing particle packing in containers with periodic boundaries, simulating infinite space, with rigid boundaries, simulating external surfaces, or with mixed conditions. Gradual reduction of the container size while particles move makes it possible achieving the high packing densities as met in practice. This is illustrated Figure 1.

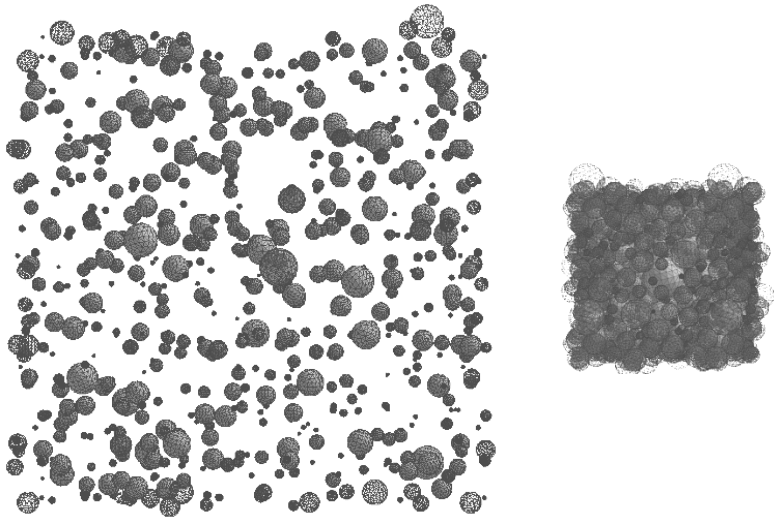

Figure 1. Spherical particles dynamically compacted from loose (left) into dense random state (right) by the DEM system HADES

2.2 ***Simulation of hydration process***

In this research, a new numerical multi-phase model for simulating hydration of (blended) cement is utilized. Herein, the hydrating grains are simulated by spherical integrated particles based on the so called 'integrated particle kinetics model' (IKPM), coupling a fresh core of material and its hydration product (CSH) as a shell coating this core [8, 29, 30]. Nonetheless, different from the IKPM model that is used for only a single-phase material (C_3S), each fresh spherical core also incorporates information of its other main components, *i.e.* percentages of phases in this model. So, the model is referred to as 'extended integrated particle kinetics model' (XIPKM).

Figure 2a is an illustration of the hydration model for a blended mixture. Beside the composite/integrated PC particle (left), a mineral admixture particle is shown consisting of

silica and inert material (*e.g.*, rice husk ash – RHA). The hydration product CH (calcium hydroxide) is modeled as single spherical particles (right, at the bottom). Researches have

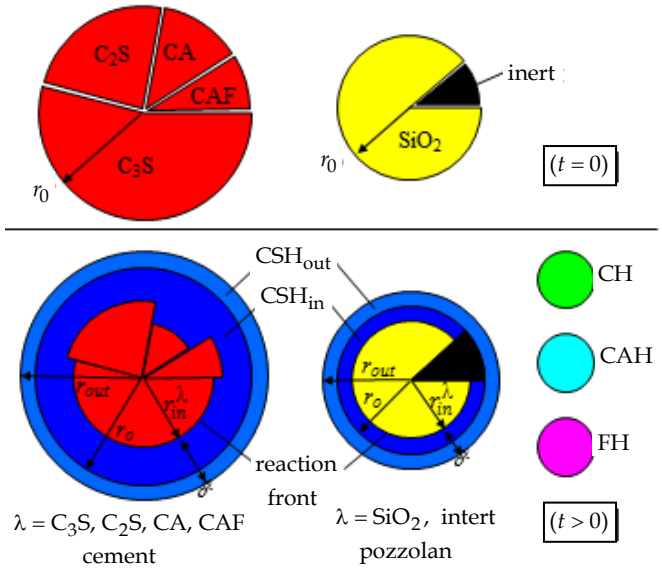

Figure 2a. 2D particle models of cement, pozzolan and hydration products in the unhydrated state (top) and the hydrated one (bottom); setup in XIPKM (short chemist notation as to cement chemistry). Note that the inner layer of CSH (CSH_{in}) compensates for the different hydration rates of the various cement compounds.

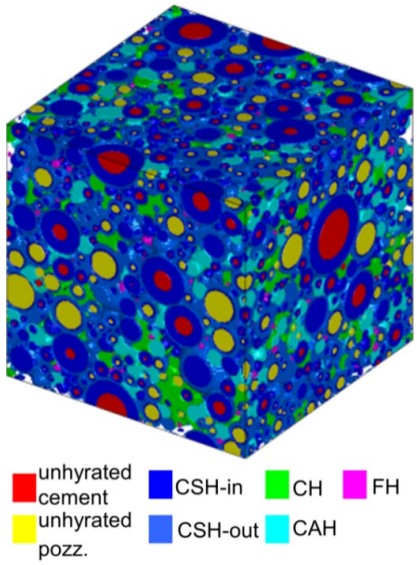

Figure 2b. Visualized hydrated microstructure

demonstrated that the CH product diffuses and nucleates randomly either in the pore space or precipitates on the surface of the existing CH grains [7]. The quality of the new hydration concept is verified on the basis of experimental data in Figure 3. Much better correspondence is found than can be expected from popular random sequential systems [12, 31].

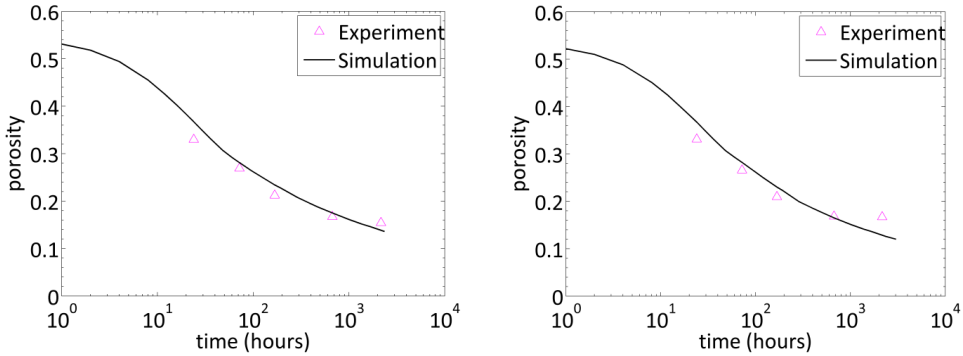

Figure 3. Porosity of the RHA-blended PC samples. The experimental results are derived from testing of Nguyen [10] on RHA-blended PC samples with w/b = 0.4 and 10% (a) and 20% (b) replacement.

2.3 ***Pore delineation by DRaMuTS***

DRaMuTS (Double Random Multiple Tree Structuring) has been introduced in [20, 21, 32, 33]. Basically, nodes are distributed uniformly random (UR) or seeded at selective places in the virtual material. A path planning algorithm is designed so that the nodes are connected by straight lines resulting in the formation of a "tree". This can be achieved starting from multiple sources, leading to multiple tree structuring. When a straight line between neighboring nodes is obstructed, a more nearby point is selected preventing iterations, however violating the UR state. Trees can ultimately merge when similar nodes are involved. The result is in general a pore structure delineated by continuous zigzag lines inside the pores. This renders possible studying topology of the pore system, so that pores connecting external surfaces of the simulated cube specimens (trunks or main channels) can be distinguished from dead-end pores connected to such trunks (the branches) and from isolated pores. The number of trees is a reflection of pore fractionation: it represents the number of transport routes through the specimen. The expansion of the trees by DRaMuTS is shown in Figure 4.

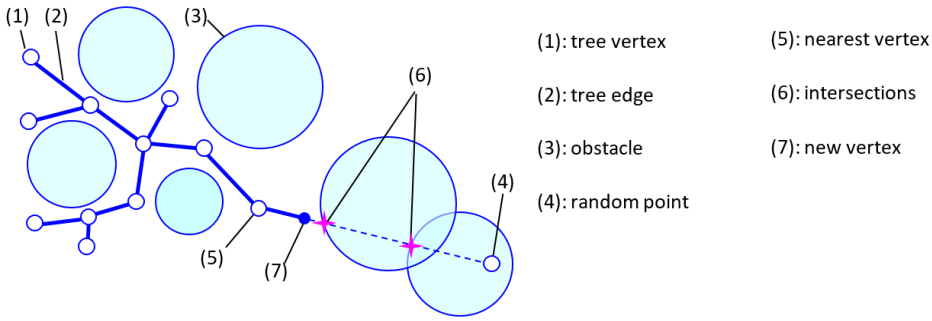

Figure 4. Path finding in robotics (RRT) is modified in DRaMuTS by avoiding iterations: note the different location of (7) after failure in (4). See [32].

*2.4 **Pore measuring by SVM***

A second UR point system is thereupon generated (note "Double Random" in DRaMuTS). The node fraction inside the pores directly governs porosity because point fraction is an unbiased estimator of volume fraction. All points inside the pores are thereupon provided with pikes in systematically arranged directions (the stars). The pikes connect the relevant node with the pore surface in the given direction. By averaging all cubed values of pike length in a point and thereupon taking the 3rd root, a measure is obtained for the local pore radius of a representative sphere, *i.e.*, a sphere with the same volume as the pore locally has. This is the so-called star volume method that can also be instrumental for obtaining this 3D information from 2D sections [20,21,34]. By combining all these local pore size measures, a volume-based pore size distribution function (PoSD) is straight-forwardly obtained.

Alternatively, in each of the random points inside the pore network, isotropic uniformly random (IUR) planes can be considered. Application of the star volume method in the plane renders possible determining the radius of a representative circle with the same area as the pore locally has. The smallest among the radii in a point is associated with local pore throat size. It can also be used for the construction of a pore *throat* size distribution. This is a more realistic measure for modeling transport through the pore. In addition to size, pore length can be considered a relevant measure in transport models. For that purpose, the somewhat zig-zag shaped tree branches and channels as depicted by Figure 5 are smoothed by a mathematical algorithm [7, 21].

The number of edges in DRaMuTS (or the number of network points, nodes) governs sensitivity. An increased density of points raises the chances of sampling very fine pores. Hydraulic arguments should be employed to decide upon the minimum pore throat size considered in the pore network structure. By gradually increasing this cut-off (minimum) pore throat size, finally the pore depercolation limit is achieved, *i.e.* the stage whereby the network structure becomes fully de-percolated. Sensitivity analyses have shown that a sufficient sensitivity level can be achieved at 10^5 points for a 100 µm cubed hardened cement paste structure. Thereupon, an increasing number of points will not significantly improve the structural estimate because of having reached a plateau value. Application of this methodology to blended cements will reveal the impact of the particle size distributions involved, in particular of the gap in median particle sizes, on the packing density which is the basis for strength development.

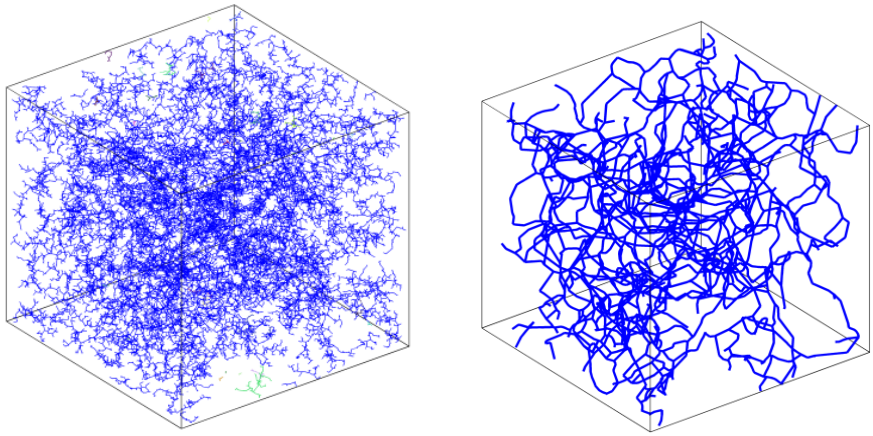

Figure 5. (left) Pore delineation in 100 µm cubes of 90 days old hydrated cement paste with w/c = 0.4 and Blaine surface area of 300 m²/kg. Porosity is 19%. (right) Only main pore channels of the same cement paste are displayed.

2.5 ***Permeability methodology***

The tube network model approach is used for estimating permeability. The methodology is extensively described in [7] to which the interested reader is referred. Basically, the network mimics the structure of main pore channels as shown in Figure 5. The tubes are cylindrical, *size* being governed by local throat observations, however the conductance is reduced due to the irregular *shape* of the pores. This reduction factor is determined by FET, as depicted in Figure 6 for a randomly selected pore throat.

3 Blending effects on strength

3.1 Strength testing

The RHA is produced in the traditional way from Vietnamese rice husks and grinded until its internal micro-porous structure collapsed, significantly reducing water demand [2]. Mean particle size was 5 µm. For additional details, see [2, 35]. Of course, the RHA grains will still contain nano-pores [9, 10]. 70% crushed basalt and 30% of fine sand of fluvial origin constituted a gap-graded aggregate mixture. 500 to 550 kg/m^3 Portland cement of two qualities were used. Three water/binder ratios (w/b) were investigated and replacement percentages of 10, 20 and 30 were envisaged. Naphthalene-based superplasticizer additions were employed to get cohesive mixtures with high slump values. 100 mm cubes were used for compressive strength testing at different stages of maturation. Detailed test results have been published in the aforementioned publications. However, Figure 7 reveals the blending efficiency resulting from gap-grading in the blends that is only revealed when RHA is combined with the coarser cement (PC30). Since strength is improved due to increase in PC quality, the results in Figure 7 are presented in relative terms.

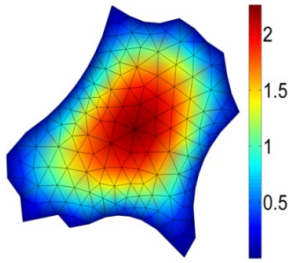

Figure 6. Shape of randomly selected pore throat, of which the conductance inefficiency (versus the representative circle) is determined by averaging the flow pattern obtained by FET over the throat area.

3.2 Strength simulation

Figure 8 presents computer simulation data revealing gradient structures of λ^{-3} values obtained by the concurrent algorithm-based DEM system SPACE [14]. Herein, λ is the mean free surface-to-surface spacing of the binder grains. This value is supposedly proportional to physical (van der Waals) strength. The normalized values for the *coarsest* cement demonstrate the far more efficient packing in the gap-graded case for 10% cement replacement. At higher dosage this effect of optimized packing is absent. Nevertheless,

concrete with low CO_2 footprint could be produced with high dosage of fine-grained RHA without *loss* of strength.

Note that pozzolanity is absent in Figure 8. The demonstrated sole effect of *particle packing* was also revealed by physical tests [6]. Herein, gap-graded blending with carbon black (inert filler!) yielded proper strength results, whereby for well-designed concretes the loss of chemical strength (as in the case of RHA blending) was compensated for by the physical strength contributions. This was confirmed in earlier experimental research efforts, in

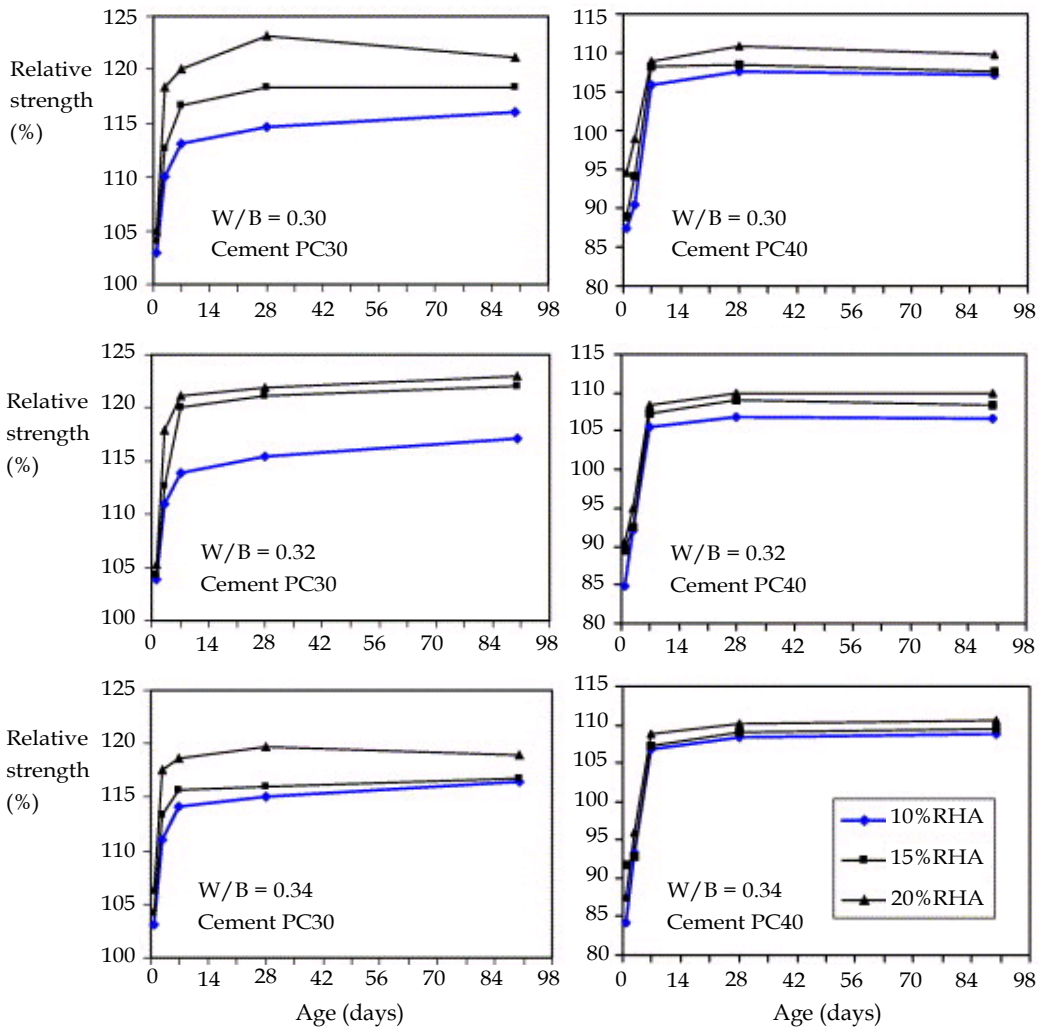

Figure 7. Relative compressive strength values of gap-graded aggregate RHA-blended concrete [2]

which we found compressive strength of blended concrete mixtures with incinerated diatomite earth (D) not to underscore meta-kaolin-blended mixtures (MK). In these experiments, diatomite is the finer admixture (D: 71.4% and MK: 42.8% finer than 5 μm) and thus yields better packing of the binder grains [36]. Both admixtures were locally produced from clays yielding only high pozzolanity of K.

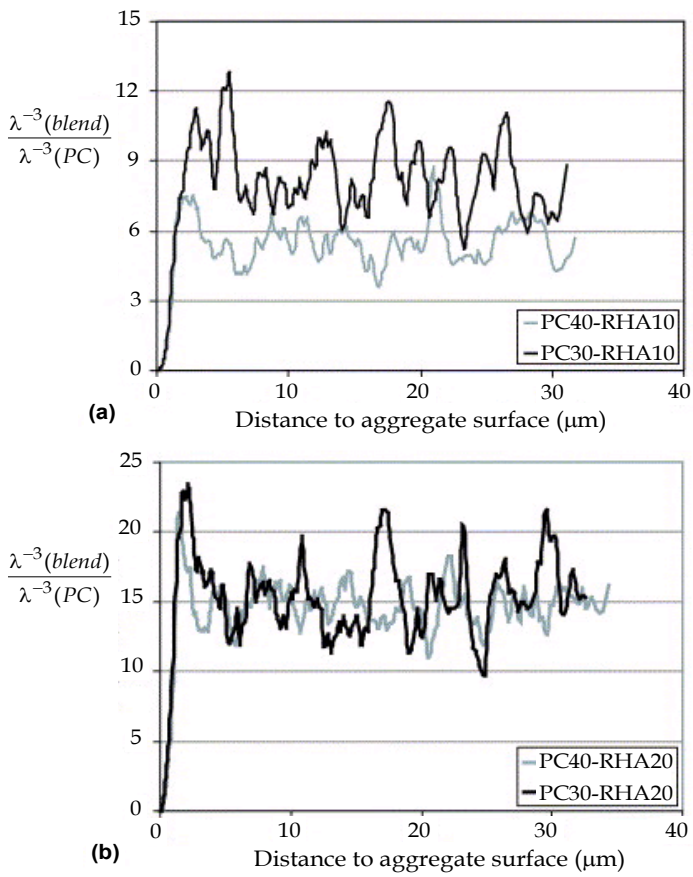

Figure 8. RHA blending reveals increased density in virtual concrete when gap-graded with the coarser PC. λ^{-3} is supposedly proportional to global van der Waals bond, whereby λ is the mean (inter-particle) free spacing.

Packing density of the aggregate as well as of the binder is directly linked up with strength. This can readily be approached in virtual reality. The alternative of experimental testing is relatively simple; however, it is more time-consuming and expensive. Yet,

transport-based durability issues are far more complicated to investigate. This paper therefore reveals an economic and also reliable way of approaching such problems in virtual reality. The most recent improvements in the virtual approach would make it possible to bridge the expected modest gap between numerical estimates and experimental permeability results, thereby accounting for involved biases related to the experiments and the actual uncertain physical state of the specimens (water saturation degree). For detailed and actual discussions on validation problems, see [38].

4 Gap-grading efficiency for material structure at different fineness

The simulation study was executed in two stages. In stage I, the impact of material parameters (*w/c* ratio, cement and RHA fineness, and particle size range) on structural characteristics were emphasized. In stage II, the optimum case from state I was studied. Particular focus was on pore geometry and topology and their consequences for water permeability were investigated.

4.1 Materials and simulation results on fineness

Cement composition: 100% C_3S

Blain fineness 300 m^2/kg

Rosin Rammler particle size distribution (n = 1.107 and b = 0.023)

Cem 133: particle size range 1~33 µm

Cem 333: particle size range 3~33 µm

Cem 350: particle size range 3~50 µm

RHA [2]:

RHA14: grinding time 14 hours

RHA18: grinding time 18 hours

RHA18+: grinding time 18 hours with grinding aid

The fineness of the model cement was influenced by the particle range (leading to increasing values in median particle size from Cem 133 to Cem 350). The fineness of the RHA is promoted by grinding duration and addition of grinding aid – for details see [2, 35, 37]. Figure 9 at the top reflects this increased fineness with grinding duration.

Figure 9 reveals the modifications in median particle size $D_{0.5}^{pa}$ as a result of varying blending doses and cement and RHA fineness (other parameters being constant).

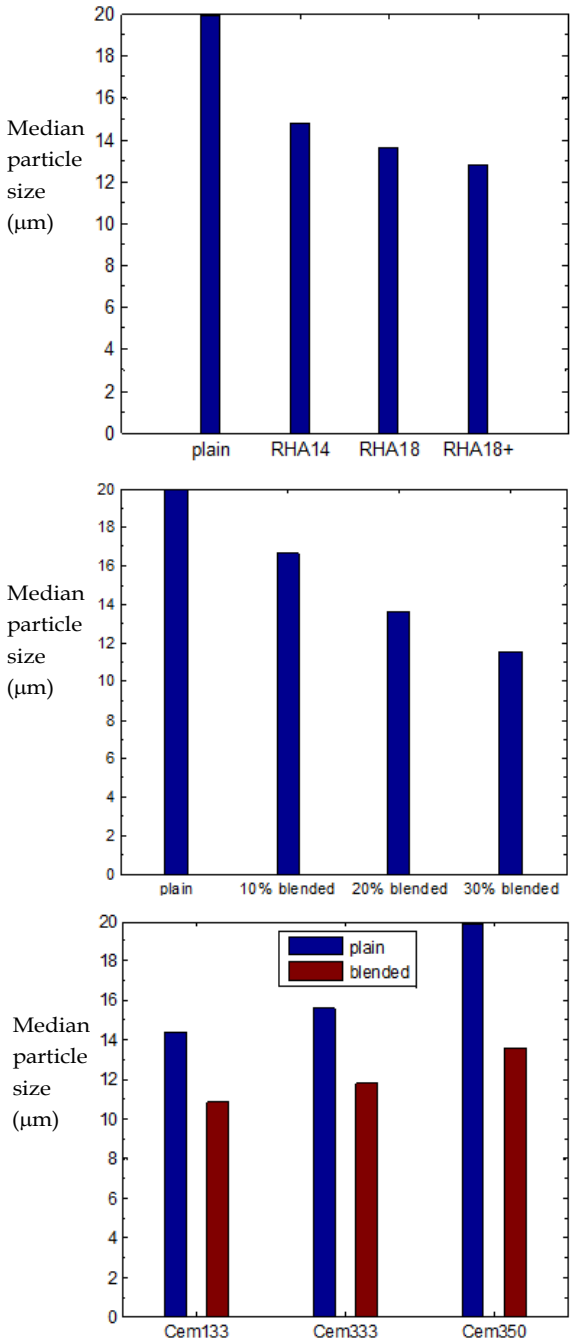

Figure 9. Median particle size of paste samples as influenced by type of RHA (top) (w/b = 0.4, Cem 350, 20% replacement), by blending percentage (middle) (RHA18, Cem 350, w/b = 0.4), and by type of cement (bottom) (w/b = 0.4, RHA18, 20% replacement).

Obviously, $D_{0.5}^{pa}$ decreases with increasing replacement percentage of the blend and increasing fineness of the RHA. In all cases this is due to the cement being coarser than the RHA. The gap between the median particle sizes of the cement and the RHA is varying leading to various degrees of packing efficiency. The gap is largest for C 350 and RHA18 in Figure 9 at the bottom, resulting in the largest median particle size decline and thus the highest packing efficiency.

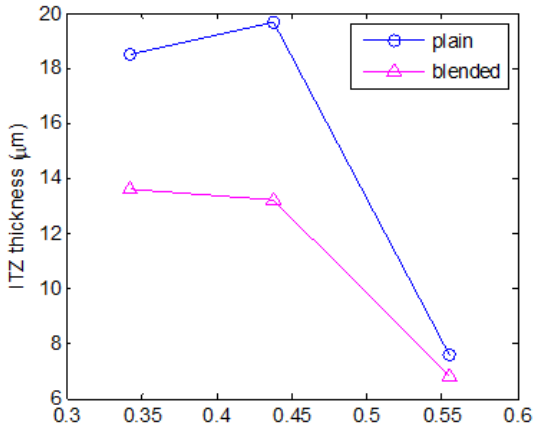

Figure 10. ITZ thickness versus initial particle volume fraction (w/b = 0.25, 0.4 and 0.6) (Cem 350, RHA18, 20% replacement)

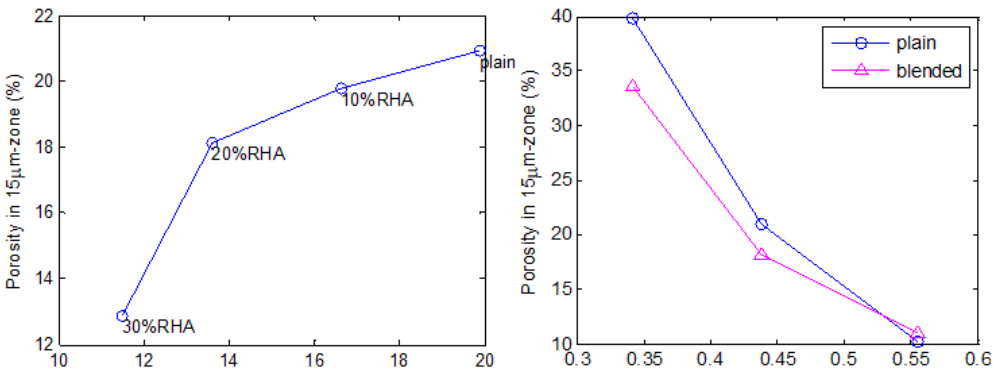

Figure 11. Left: average porosity in ITZ zone of pastes with different blending percentages (w/b = 0.4, Cem 350, RHA18) and at the right for initial particle volume fractions (w/b = 0.4, RHA18, 20% replacement)

4.2 *Results on porosity*

Cubic samples of (blended) cement paste were simulated with 100 - 150 µm side length and two opposite rigid boundaries and four periodic ones in which the particle mixtures were packed by HADES. Thereupon, hydration was by XIPKM, whereupon the structural assessment was conducted by application of DRaMuTS and SVM.

When the simulated specimens are serially sectioned, curves can be constructed of section porosity as function of the location of the section. The section porosity is calculated as the ratio of the total pore area and the total area of the section, which can be directly

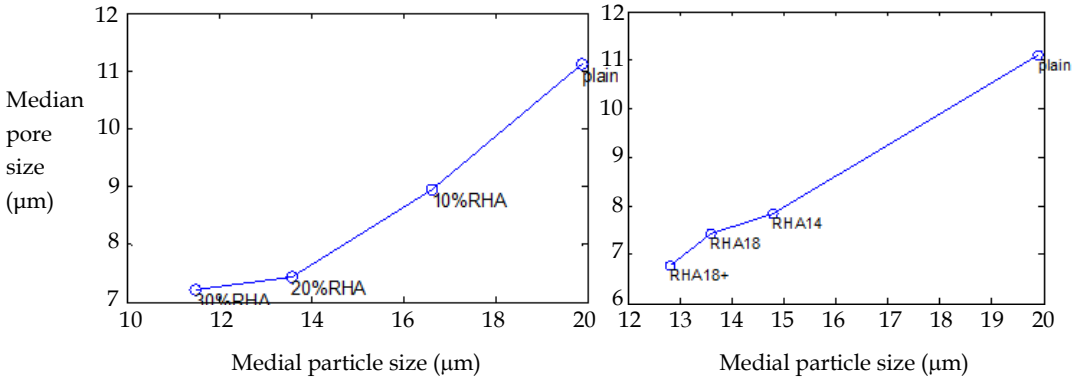

Figure 12. Left: median particle size ($D_{0.5}^{pa}$) versus median pore size ($D_{0.5}^{po}$) of pastes with different percentages of blending (w/b = 0.4, Cem350, RHA18) and at the right for different types of RHA (w/b = 0.4, Cem 350, 20% replacement)

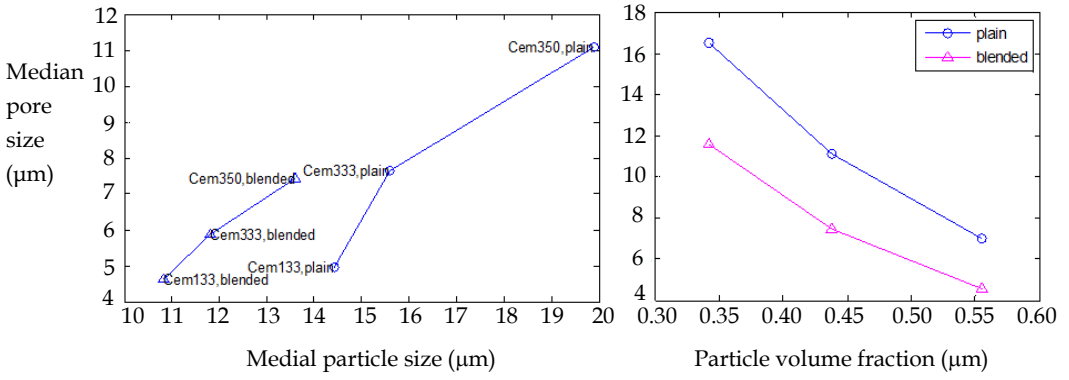

Figure 13. Left: $D_{0.5}^{pa}$ versus $D_{0.5}^{po}$ of plain and blended samples with different cement particle size ranges (w/b = 0.4, RHA18, 20% replacement) and at the right with different w/b ratios (Cem 350, RHA18, 20% replacement)

interpreted in 3D terms. In general, a zone with higher porosity adjacent to the aggregate grain surface is reduced in thickness due to blending. This is the so-called Interfacial Transition Zone (ITZ) for porosity. To characterize the effect of RHA blending on the presented pore characteristics, the median pore size $D_{0.5}^{po}$ is used in combination with $D_{0.5}^{pa}$ that characterizes the median particle size of the designed binder.

Average porosity in a 15 µm wide zone adjacent to the aggregate grain surface (supposedly approximating the ITZ) was found almost linearly declining with blending percentage (*w/b* = 0.4, Cem 350, RHA18), with RHA fineness (*w/b* = 0.4, Cem 350, 20% replacement), with cement fineness (*w/b* = 0.4, RHA18, 20% replacement) and also for particle volume fraction (*w/b* = 0.4, RHA18, 20% replacement), as illustrated in Figures 10 - 14. Hence, this effect of ITZ reduction is largest at a *maximum gap between the median grain sizes of the cement (C350) and of the RHA (RHA18+)*. This is the result of more efficient packing due to size segregation, which will be promoted by a higher *w/b* ratio.

So, a gap-graded particle design of the binder can reduce the extent of the relatively highly porous ITZ as well as reducing the involved pore sizes (Fig. 14). This will have a favourable effect on permeability as will be demonstrated by the second set of experiments.

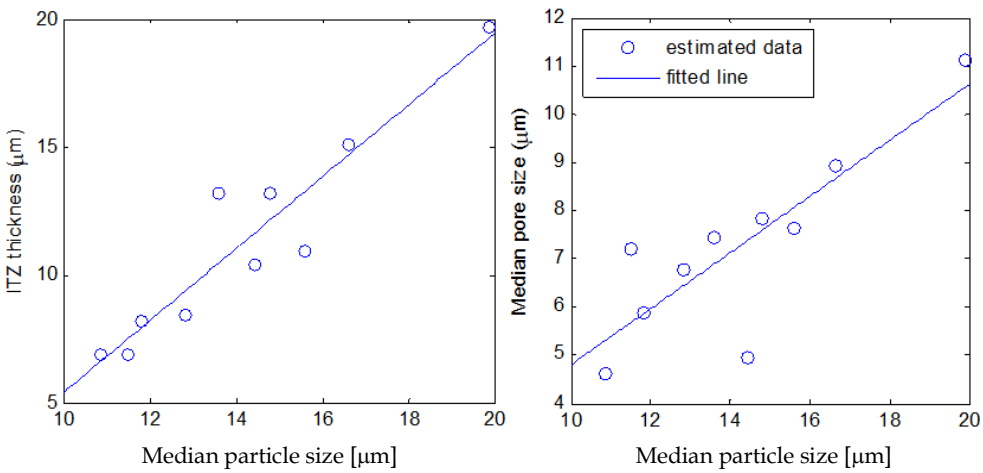

Figure 14. Linear regression for ITZ thickness (left) and for $D_{0.5}^{po}$ (right) both as function of $D_{0.5}^{pa}$; based on data of samples with w/b = 0.4

5 Gap-grading efficiency for pore permeability at optimum fineness

5.1 Input parameters

Various plain and pozzolanic-blended cement specimens are used to investigate the influence of different input parameters, *i.e.*, *w/b* ratio, cement fineness, and blending dosage on the pore characteristics. The material properties of cement and pozzolanic admixture and the corresponding input parameters for simulating the microstructural evolution during hydration are given in Table 1. The reference pozzolanic admixture is the Vietnamese rice husk ash leading to optimum gap graded conditions in section 4, and is designated as RHA18+. Properties and production procedure are detailed in Bui (2001) [2]. As an example, for the notation used for mixtures, W40F300R20 is the code of a blended specimen with *w/b* = 0.4, cement fineness of 300 m²/kg and 20% RHA blending. The specimens are simulated in a cubic container with two rigid walls and four periodic ones to simulate the paste zones (involving ITZ and bulk zones) between the aggregates' surfaces. The procedure for reducing the particle size range and the assessment of particle numbers of the model specimens are described in (Le, 2015) [7].

5.2 Porosity evolution during hydration

The global porosity evolution of the plain and blended cement specimens are shown in Figure 15. Blending has the most significant effect on reducing global porosity at an advanced state of hydration. This is most obvious at higher *w/b* ratio. The RHA-blending

Table 1. Material properties and their corresponding simulation input data

Materials	Cement I	Cement II	Pozzolanic admixture
Type	Portland	Portland	**RHA18+**
Cement fineness (m²/kg)	300	550	-
f_0 - C_3S:C_2S:C3A:C_4AF	0.542:0.278:0.064:0.117	0.649:0.193:0.081:0.078	-
b, *n* – cement	0.023, 1.107	0.067, 1.03	
Size range (μm)	0.41 - 33	0.21 - 33	0.01 - 17.70
K_0 - C_3S; C_2S;	0.0557; 0.0064;	0.0513; 0.0064;	-
C_3A; C_4AF (μm/h)	0.0373; 0.0056	0.0373; 0.0056	-
K_0 - RHA (μm/h)	-	-	0.007
Container size: 100x100x100 (μm)			

b and *n* are the constants of the Rosin-Rammler particle size distribution function.

K_0 is the expansion rate due to water consumption. For details, see [7].

dosage is the percentage by weight of the replaced amount of cement. Since the specific density of RHA is smaller than that of cement, partial cement replacement leads to an increase in the total volume of the solid phases. This automatically causes a reduction in the capillary porosity of blended pastes with respect to the plain paste at equal *w/b* ratio even before hydration ($t = 0$).

5.3 Porosity gradient

The smoothed functions in Figure 15 [7] are the sectional porosity gradients of the specimens at 90 days of hydration. The sectional porosity represents the pore fraction in a thin slice parallel to the rigid wall at a given distance to that wall. From the gradient functions, the ITZ/bulk boundaries of the specimens can be obtained. The ITZ thickness obtained this way was used in Figure 14. The ITZ thickness is demonstrated increasing with the higher *w/c* for plain cement paste, however there is not a clear trend exerted by blending on the ITZ thickness. It should be recalled that the virtual cement that is investigated is finer-grained than the real cement. Hence, the ITZ thickness is proportionally reduced.

5.4 Pore size distribution

With the eye on use of the pore size characteristics in a transport-based model, the pore size distribution (PoSD) will be based on the *smallest pore sections (throats)*. The evolution in

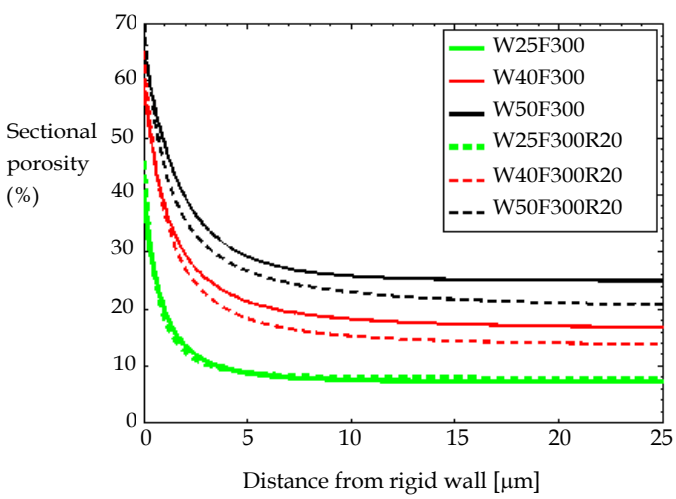

Figure 15. Porosity gradient in direction perpendicular to rigid surfaces of specimens; 90 days hydrated

the pore size distribution (PoSD) of the plain versus the blended specimens with *w/b* = 0.4 is presented in Figure 16. The blending efficiency is revealed by the shift of the PoSD function to the left (*i.e.*, a reduction in pore sizes) at an early stage of hydration. Furthermore, the PoSD of the plain specimen is modified significantly from 7 to 365 days of hydration. From the above investigations, it can be concluded that blending significantly reduces the pore size in a specimen. In addition to that, the global porosity is reduced as well, as shown in [7].

5.5 ***Permeability***

Figure 17 (left) depicts the evolution in permeability during hydration of the plain and blended specimens with *w/b* = 0.4. The permeability in the plain paste declines gradually and significantly for a long period of time from early hydration. On the contrary, the efficiency of blending is revealed by a much lower permeability of the blended specimen at early hydration that diminishes only marginally after 28 days of hydration. At the right, the permeability is shown of the plain and blended cement pastes with different *w/b* ratios; the blending impact on permeability of the specimens is obvious. Figure 18 (left) presents the influence of the blending percentage on the permeability. The different plain and blended specimens are investigated at the same porosity. A reduction in permeability is revealed at increasing blending dosage. However, the permeability of the blended paste does not change significantly from 20% to 30% dosage. Figure 18 (right) shows the

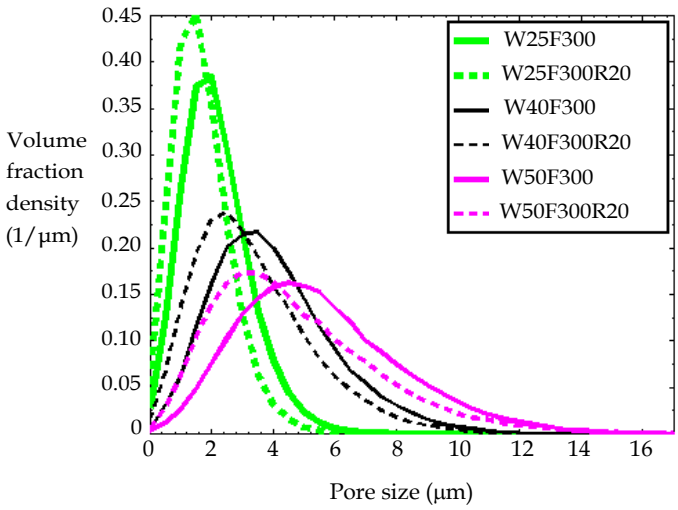

Figure 16. Evolution of the pore size distribution during 7, 28, 90 and 365 days of hydration in plain and blended specimens with w/b = 0.4

permeability of the plain and blended cement pastes with different cement fineness. The blending effect, again, is not revealed for the cement paste with the higher fineness. This is due to the aforementioned perturbation effect in particle packing.

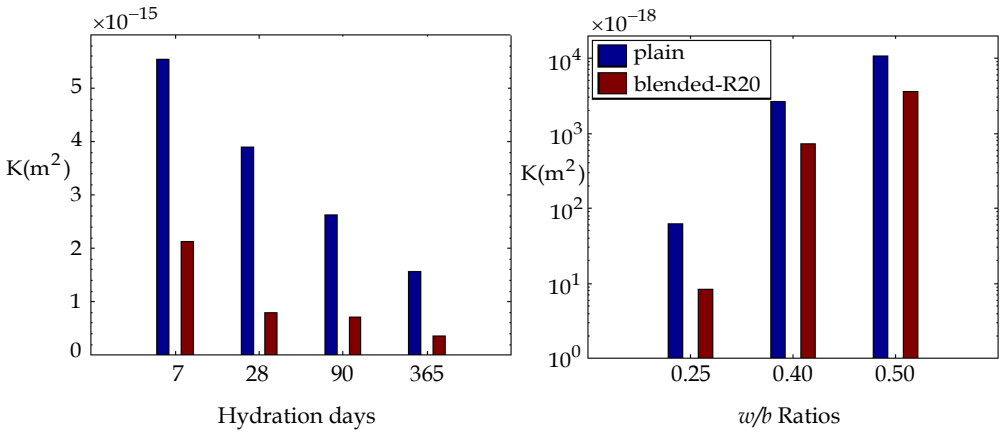

Figure 17. (left) Evolution of permeability during hydration in 7, 28, 90 and 365 days of plain and blended specimens with w/b = 0.4. (right) Permeability of plain versus blended specimens with different w/b ratios at 90 days of hydration

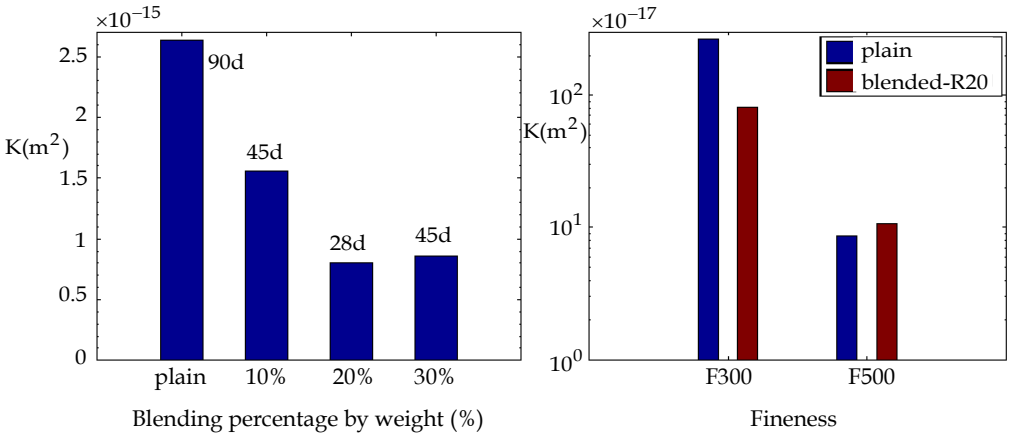

Figure 18. (left) Permeability of blended specimens with different replacement percentages at the same porosity (≈18%). (right) Permeability of plain versus blended specimens with different cement fineness at the same porosity (≈18%) and w/b = 0.4

6 Discussion and conclusions

This study investigated the effects of RHA blending on structural characteristics (density, presumably related to compressive strength, extension of the ITZ). In a second stage also water permeability was investigated in blended specimens. For that purpose, input parameters were varied, such as blending percentage, fineness of the RHA, fineness of the cement and the *w/b* ratio. The investigated parameters can be assumed the major ones governing strength and transport capacity of the cementitious materials. The investigated quantities are shown as function of the median particle size $D_{0.5}^{pa}$. Similarly, the resulting pore characteristics are contracted into the median pore size $D_{0.5}^{po}$. This rendered possible revealing the blending effect in the experimental set ups. Moreover, it avoids computational problems due to too large particle numbers or particle ranges.

For example, ITZ thickness and $D_{0.5}^{po}$ are formulated as functions of $D_{0.5}^{pa}$ by linear regression from the obtained data collected of the different samples. The extent of the ITZ cannot unambiguously be assessed. In this study the pore location distribution is approximated by an exponential function, whereupon the ITZ thickness is determined as the distance from the rigid wall to the point where the function approaches a plateau value (hence, porosity merges into bulk value).

The approach by dynamic, force-based DEM (HADES), XIPKM, DRaMuTS and SVM, briefly introduced herein, constitutes an economic and reliable way of investigating structural problems of cementitious materials, as extensively discussed in the international literature, such as in [12, 38]. Particularly, topology and geometry of the complex and tortuous pore network structure, which are at the basis of (polluted) water transport related durability properties, are readily obtained. For that purpose, the fresh DEM-simulated particle structure is hydrated by XIPKM, which is able considering the major compounds of the PC as well as particles of a mineral admixture by which the cement is blended for promoting low CO_2 concretes. Application to gap-graded RHA-blended PC has confirmed the favorable effects on packing density, which is related to strength. Moreover, it has revealed a pore refinement in general as well as in an ITZ of reduced extension. Hence, permeability is also reduced, which will have a positive impact on (polluted) water related durability and thus also on these aspects of service life.

A final remark for correct interpretation of the paper. Strength results were derived from physical experiments on *concrete* containing gap-graded RHA-blended cement and obtained in Delft with Vietnamese PhD students. Results of virtual experiments conducted in Delft with additional Vietnamese and Chinese PhD students were however on (blended) *cement paste*. The prime target of the paper was focusing on the particle packing impact on permeability. The data transfer from cement paste to concrete can be made by accounting for the aggregate dilution and the pore tortuosity effect exerted by the aggregate in normal concrete. Comparisons with outcomes presented in the literature is frustrated by most *virtual approaches* being based on RSA instead of DEM particle packing [12]. Further complications are the result of *physical experiments* on concrete conducted by MIP and by dealing unintentionally with both micro-cracking and additionally with not fully water saturated material, both to an unknown degree [18, 24]. In partially water saturated conditions, more representative for the *engineering field*, the ITZ was shown having just marginal impact [26].

Acknowledgement

The results of a continuing study into particle packing effects on sustainability-promoting properties of (blended) Portland cement concrete were fostered by a sequence of PhD studies at our university, *i.e.*, Martijn Stroeven, Danh Dai Bui, Dinh Dau Vu, Jing Hu, Huan He, Luong Bao Nghi Le, and Kai Li. Their significant contributions are highly acknowledged. Further, these studies were supported by the Royal Academy of Arts and Sciences (KNAW), the Dutch Organization for Internationalization in Education (NUFFIC), Dgis (Ministry of Development Cooperation), the Research Fellowship Program of DUT, and Vietnamese and Chinese Educational Ministries. They guaranteed the progress in this also worldwide actual research field. Therefore, with gratitude we have welcomed and still highly appreciate their financial support.

References

[1] Stroeven, P., Dalhuisen, D.H., Nguyen, T.Q., Bui, D.D., Dong, V.A. (1995) "Toward gap-graded HPC in Vietnam using crushed rock, very fine sand and RHA-blended cement", In: 2*nd CANMET/ACI Int. Symp. Advances in Concrete Technology*, Ottawa, Canada, SP-154-14, Nat. Resources. pp. 263-278

[2] Bui, D.D. (2001) "*Rice husk ash as a mineral admixture for high performance concrete*", PhD Thesis, Delft University of Technology

[3] Vu, D.D. (2002) "*Strength properties of metakaolin-blended paste, mortar and concrete*", PhD Thesis, Delft University of Technology

[4] Bui, D.D., Stroeven, P. (1996) "Experimental assessment of the development potentialities of cement-based building materials in Vietnam using indigenous resources". In: *Proc. XXIV IAHS World Housing Congress*, Ankara, pp. 1082-1093.

[5] Detwiler, R.J., Mehta, P.K. (1989) "Chemical and Physical Effects of Silica Fume on the Mechanical Behavior of Concrete", *ACI Mat. J.*, 86(6): 609-614

[6] Goldman, A., Bentur, A. (1993) "The influence of microfillers on enhancement of concrete strength", *Cem. Concr. Res.*, 23(4): 962-972

[7] Le, L.B.N. (2015) "*Micro-level porosimetry of virtual cementitious materials - structural impact on mechanical and durability evolution*", PhD Thesis, Delft University of Technology.

[8] Le, L.B.N., Stroeven, P. (2012) "Strength and durability evaluation by DEM approach of green concrete based on gap-graded cement blending", *Adv. Mat. Res.*, 450-451: 631-640

[9] Nguyen, V.P. (2011) "*Multi-scale failure modelling of quasi-brittle materials*", PhD Thesis, Delft University of Technology

[10] Nguyen, V.T. (2011) "*Rice husk ash as a mineral admixture for ultra high performance concrete*", PhD Thesis, Delft University of Technology

[11] Stroeven, P., He, H. (2014) "Concrete, from a centuries-old construction material to modern particle-based composite concepts", In: *Particulate Products, Tailoring Properties for Optimal Performance*, Merkus, H.G., Meesters, G.M.H., Eds., Dordrecht, Springer, pp. 209-252

[12] Li, K., Stroeven, P. (2018) "RSA vs DEM in view of particle packing-related properties of cementitious materials". *Comp. Concr.*, 22(1): 83-91

[13] Stroeven, P., Hu, J., Stroeven, M. (2009) "On the usefulness of discrete element computer modeling of particle packing for material characterization in concrete technology", *Comp. Concr.*, 6(2): 133-153

[14] Stroeven, M. (1999) "*Discrete numerical modelling of composite materials - application to cementitious materials*". PhD Thesis, Delft University of Technology

[15] Hu, J. (2004) "*Porosity in concrete – morphological study of model concrete*", PhD Thesis, Delft University of Technology

[16] Chen, H.S., Stroeven, P., Ye, G., Stroeven, M. (2006) "Influence of boundary conditions on pore percolation in model cement paste", *Key Engrn. Mat.*, 302-303:486-492

[17] He, H. (2010) "*Computational modelling of particle packing in concrete*", PhD Thesis, Delft University of Technology

[18] Li, K. (2017) "*Numerical determination of permeability in unsaturated cementitious materials*". PhD Thesis, Delft University of Technology.

[19] Vogel, H.J., Roth, K. (2001) "Quantitative morphology and network representation of soil pore structure", *Adv. in Water Resources.* 24(3-4): 233-242

[20] Stroeven, P., Le, L.B.N., He, H. (2012) "Methodological approaches to 3D pore structure exploration in cementitious materials", *Key Engrn. Mat.*, 517: 305-314

[21] Stroeven, P., Le, L.B.N., Sluys, L.J., He, H. (2012) "Porosimetry by double random multiple tree structuring", *Im. Anal. Stereol.*, 31: 55-63

[22] Stroeven, P., Le, N.L.B., Sluys, L.J., He, H. (2012). "Porosimetry by random node structuring in virtual concrete". *Im. Anal. Stereol.*, 31: 79-87

[23] Maghsoodi, V., Ramezanianpour, A.A. (2012) "Effects of volumetric aggregate fraction of transport properties of concrete and mortar", *Arab. J. Sci. Engrn.*, 34(2B): 327-335

[24] Li, K., Stroeven, M., Stroeven, P., Sluys, L.J. (2016) "Investigation of liquid water and gas permeability of partly saturated cement paste by DEM approach". *Cem. Concr. Res.*, 83: 104-113

[25] Li, K., Stroeven, M., Stroeven, P., Sluys, L.J. (2017) "Effects of technological parameters on permeability estimation of partly saturated cement paste by DEM approach". *Cem. Concr. Comp.*, 84: 222-231

[26] Li, K., Stroeven, P. (2017) "Systematic research on compucrete can shed light on some controversal isseus in concrete technology". *Heron*, 62(1): 47-59

[27] He, H., Le, L.B.N., Stroeven, P. (2012) "Particulate structure and microstructure evolution of concrete investigated by DEM", Part I. *Heron*, 57(2): 119-132

[28] He, H., Le, L.B.N., Stroeven, P. (2012) "Particulate structure and microstructure evolution of concrete investigated by DEM", Part II. *Heron*, 57(2): 133-150

[29] Stroeven, M., Stroeven, P. (1997) "Simulation of hydration and the formation of microstructure", In: *Computational Plasticity, Fundamentals and Applications*, Owen, D.R.J., Oñate E. and Hinton E. eds. Barcelona, Spain. pp. 981-987

[30] Le, L.B.N., Stroeven, M., Stroeven, M., Stroeven, P. (2013) "A novel numerical multi-component model for simulating hydration of cement", *Comp. Mat. Sci.*, 78: 12-21

[31] Williams, S.R. and Philipse, A.P. (2003) "Random packings of spheres and spherocylinders simulated by mechanical contraction". *Phys. Rev. E-Statist., Nonlin. Soft Matter Phys.*, 67: 1-9 051301

[32] Stroeven, P., Sluys, L.J., Le, L.B.N. (2012) "Assessment of pore characteristics in virtual concrete by path planning methodology". In: *Proc. Brittle Matrix Composites 10*. A.M. Brandt, J. Olek, J.A. Glinicki, C.K.Y. Leung, eds. Woodhead Publ., Cambridge (UK), pp. 200-207

[33] Stroeven, P., Le, N.L.B., Sluys, L.J., He, H. (2012). "Porosimetry by double random multiple tree structuring". *Im. Anal. Stereol.*, 31: 55-63

[34] Gundersen, H.J.G., et al. (1988). "Some new stereological tools - and their use in pathological research and diagnosis". *Acta Pathol. Microbiol. Immun. Scand.*, 96: 379-394 and 857-881

[35] Bui, D.D., Hu, J., Stroeven, P. (2005) "Particle size effect on the strength of rice husk ash blended gap-graded Portland cement concrete", *Cem. Concr. Comp.*, 27(3): 357-366

[36] Stroeven, P., Vu, D.D. (1998) "Strength of diatomite- and kaolin-blended Portland cement pastes and concretes", In: *Material Science and Concrete Properties, 1st Int. Meeting*, Toulouse, France, 5-6 March, INSA, Toulouse, pp. 11-18

[37] Stroeven, P., Bui, D.D., Sabuni, E.L. (1999) "Ash of vegetable waste used for economic production of low and high strength hydraulic binders", *Fuel*, 78: 153-159

[38] Stroeven, P., Li, K. (2020) "Modern approach to surface layer modifications of hydrated cement paste for improving permeability estimates of virtual concrete", *Heron*, 65(3): 187-206